

Benchmarking Hebbian learning rules for associative memory

Anders Lansner^{1,2}, Naresh B Ravichandran¹, Paweł Herman^{1,3}

Corresponding author: Anders Lansner, ala@kth.se

¹KTH Royal Institute of Technology, EECS

²Stockholm University, Mathematics

³Digital Futures, KTH Royal Institute of Technology

Abstract

Associative memory or content addressable memory is an important component function in computer science and information processing and is a key concept in cognitive and computational brain science. Many different neural network architectures and learning rules have been proposed to model the brain's associative memory while investigating key functions like pattern completion and rivalry, noise reduction, and storage capacity. A less investigated but important function is prototype extraction where the training set comprises pattern instances generated by distorting prototype patterns and the task of the trained network is to recall the correct prototype pattern given a new instance. In this paper we characterize these different aspects of associative memory performance and benchmark six different learning rules on storage capacity and prototype extraction. We consider only models with Hebbian plasticity that operate on sparse distributed representations with unit activities in the interval [0,1]. We evaluate both non-modular and modular network architectures and compare performance when trained and tested on different kinds of sparse random binary pattern sets, including correlated ones. We show that covariance learning has a robust but low storage capacity under these conditions and that the Bayesian Confidence Propagation learning rule (BCPNN) is superior with a good margin in all cases except one, reaching a three times higher composite score than the second best learning rule tested.

Keywords: Associative memory, content addressable memory, benchmarks, Hebbian learning rules, modular neural network, storage capacity, prototype extraction, performance scaling.

Introduction

Associative memory as a concept in computer science refers to a memory that is content addressable, i.e., able to retrieve a stored item when given a fragment or distorted copy of it or to retrieve an item when cued by another associated item. Such so called auto- and hetero-association respectively, also reflect the meaning of associative memory in cognitive brain science and psychology. There, autoassociative memory in recurrent cortical neural networks is thought to underlie fundamental processes and brain computations like, for instance, figure-

ground segmentation, long-term memory, perceptual completion and rivalry. Key elements of stimulus-response behavior and associative chaining based thought processes are described as heteroassociative, with a stimulus item associated to e.g. an action or successor in a sequence. The search for the neural mechanisms behind associative memory dates back at least to the works of Donald Hebb and his cell assembly theory and hypotheses about mental representations in the form of cell assemblies and memory based on synaptic associative, i.e. “Hebbian”, plasticity (Hebb, 1949).

The focus of this paper is on brain modeling and machine learning aspects of one-layer autoassociative memory and related neuroscientific theories and computational models. Following (Palm (2013), the term “neural associative memory” (NAM) is adopted to distinguish such neurally oriented models of associative memory from more abstract ones studied in cognitive science and from other common types of error-correction based artificial neural networks. Further, since error-correction based learning is still not accepted as biologically plausible, we here restrict our investigation to different variants of Hebbian learning rules proposed for associative memory. Our aim is to compare quantitatively the associative memory performance of different NAM models by means of a set of benchmark tasks. We emphasize the influence of the learning rule employed by implementing a generic and as simple as possible network architectures including activation functions.

The so called modern Hopfield networks are interesting extensions of their classical counterpart, which gains performance by introducing stronger non-linearities into the associative processing (Krotov & Hopfield, 2019). This introduces some form of hidden layer with a complex higher order internal representation. Such models are beyond the scope of the simpler one-layer architectures in focus here which, however, recently have been extended in a similar direction and applied to machine learning benchmarks (Ravichandran et al., 2020).

Associative memory and pattern reconstruction

An autoassociative memory is essentially a memory that is content addressable in the sense that when stimulated with some input pattern the most similar among the stored patterns is recalled. In the linear forms of “matrix memories” the patterns are simply vectors with real valued components. However, more commonly the patterns are binary and have components $\{0,1\}$ or $\{-1,1\}$ or with continuous-valued activation in the corresponding interval, e.g. $[0,1]$. Neuron spiking frequency when subject to sensory input may be considered as a confidence of the key stimulus being present (Meyniel et al., 2015). The pattern format that comes closest to this view is one with components in some interval between zero and maximal firing frequency, possibly normalized to $[0,1]$. It is thus somewhat surprising that much work in the NAM field has used and still uses the bipolar pattern activation function, possibly due to the strong influence from spin glass physics, as noted by Palm¹.

¹Günther Palm, 2013: “... probably due to the misleading symmetry assumption (symmetry with respect to sign change) that was imported from spin-glass physics. This prevented the use of binary $\{0, 1\}$ activity values and the corresponding Hebb rule and the discovery of sparseness.”

Proper function of the associative pattern processing in the neural network requires that the memory is not overloaded. When too many patterns are stored in a fixed size network, memory function typically breaks down and recalled patterns become distorted or may even be spurious, without obvious relation to any of the stored patterns. Central questions in the field have been and is still what learning rule and activation function gives the highest pattern *storage capacity and scaling* to large network sizes, as well as how to avoid the above mentioned so called “catastrophic forgetting” (Burgess et al., 1991). This is the main subject of this work where we compare by computational experiments how the storage capacity depends on the learning rule used.

Another interesting but less well studied operation of NAM:s is that of *prototype extraction*. It emerges when training the associative memory network with a number of pattern instances generated from one of a set of prototype patterns by adding some form of distortions. When recall is tested with new instances, the memory is expected to recall the most similar prototype pattern, which itself was never presented to the network. Such an operation is closely related to clustering in data science and to concept and category formation in humans. Work on such learning in ANN has been scarce, but see e.g. Amari (1977), Lansner (1985, 1986) and recent modeling of such operations in ANN (Ross et al., 2017; Tamosiunaite et al., 2022) and human concept formation (Fernandino et al., 2022).

Storage capacity scaling of stored patterns or of prototypes extracted from instances are the two operations for which we in the following define and demonstrate benchmarks in order to compare the capabilities of different Hebbian NAM learning rules.

Brief overview of earlier work on Neural Associative Memory

Hebb’s work and publications in the 1940’s inspired research in early theoretical and computational brain science as well as in engineering. Focus was on recurrent spiking neural network models and testing for emergence of Hebbian cell assemblies in biological tissue. As an example, early computer simulations by Rochester et al. (1956) failed to show that cell assemblies with sustained activity could form in a recurrently connected network of spiking model neurons². Other early work was on associative memory in the hippocampus (Marr, 1971) and further development of models of memory function, associative memory, and concept formation followed (see e.g. Amari, 1977, 1989; Anderson et al., 1977; Nakano, 1972).

In the electronics and computer science domain the earliest associative memory work was by Steinbuch (Steinbuch & Piske, 1963). Steinbuch’s LernMatrix was a binary or real valued crossbar associative network that took binary or normalized real valued vectors as input and produced a binary or real valued weight matrix during learning that was then used to generate output from new input. An important focus was hardware realization and several devices were produced and even used in applications. Kohonen developed further the Correlation matrix memory, quite related to the LernMatrix with real valued weights (Kohonen, 1972). Associative memory also originated early in the research community around holographic

² This was achieved only later when the neuron properties was modelled after cortical pyramidal cells instead of spinal motor neurons (Lansner, 1986).

associative memories (Gabor, 1968; Longuet-Higgins, 1968). Work by Willshaw et al. (1969) developed further the concept of the associative memory models with binary weight matrix similar to the binary LearnMatrix and it was followed by in depth analyses of the storage capacity of such NAM:s (Palm, 1980, 2013; Schwenker et al., 1996a). Important later work from the mathematical statistics and information theory perspective on structural plasticity and iterative retrieval was recently published (Knoblauch & Palm, 2020; Knoblauch & Sommer, 2016).

The interest among theoretical physicist in brain modeling and associative memory in the form of attractor neural networks was spawned by the work of Little (1974) and was popularized by Hopfield (1982) who brought into focus the analogy between spin-glass physics and brain neurodynamics. This work has been further extended and elaborated by many researchers (see e.g. Amit et al., 1987; Kanter & Sompolinsky, 1986) with the occurrence of fixpoint, line- and chaotic attractors, and phase transitions in focus.

The Bayesian Confidence Propagation Neural Network (BCPNN) was first introduced in the late 1980's (Lansner & Ekeberg, 1987, 1989) and later developed with a modular architecture of hypercolumns and minicolumns (Lansner & Holst, 1996; Sandberg et al., 2002). It has been used extensively to model cortical associative memory in non-spiking and spiking forms (Fiebig & Lansner, 2017; Lansner et al., 2013; Lundqvist et al., 2010a, 2011). The BCPNN is related to the Potts neural network with “multi-state neurons” which was introduced in the late 1980's (Kanter, 1988) and later used as an associative memory (Mari & Treves, 1998; Naim et al., 2018). Interest in this kind of modular neural network architectures has recently risen in the context of quantum computing (Fiorelli et al., 2022).

Methods

Network architectures, selected learning rules, and delimitations

Associative memory network models typically have a simple architecture often with just one recurrent layer, sometimes two or more. For this work we used such a one-layer architecture having units with binary output operating on sparse, distributed activity patterns. Unit activation functions could take many forms, but for simplicity we used only winner-take-all (WTA) variants.

Two network versions were considered, a non-modular one with N units, designated “KofN”, and a modular one having H modules (“hypercolumns”) with M units (“minicolumns”) each, designated as “ $H \times M$ ”. For the non-modular network we used a k -winners-take-all, kWTA, activation function. In the modular network, each module used a local WTA activation function. For this kind of modular network, the partitioning of the N units can be done in many ways, but we here followed the “small world” scheme, $H = M = \sqrt{N}$, proposed for cortex long ago by Braitenberg (1978). This is reasonable, at least for the relatively small network sizes considered here.

Notably, from a neurobiological point of view, the modular network seems straight-forward to realize with local lateral inhibition and divisive normalization provided by basket cells (Carandini et al., 1997; Lundqvist et al., 2010b), whereas the kWTA selection of maximally active units over the entire network is more problematic to map to neocortical architecture.

Also, in both cases, the fixed number of active units in patterns is a strong and quite unnatural constraint. Other more capable and biologically plausible schemes have been proposed and evaluated, but for our purpose here of comparing different learning rules we judged the simplest activation functions to be most appropriate. We also employed iterative updating which is known to enhance recall (Schwenker et al. 1996).

In our comparison, we consider only local learning rules of a Hebbian correlation-based type, which can be expressed by simple probabilistic measures of neuron activity and co-activity available at the synapse (Gerstner et al., 2014; Minai, 1997; Stuchlik, 2014). We include also rules that feature intrinsic plasticity, i.e. an activity dependent regulation of unit baseline activity as has been described experimentally (Egorov et al., 2002). In this study, we have included six learning rules according to this list:

1. The *Willshaw* learning rule proposed by Willshaw et al. (1969) based on earlier work by Steinbuch and later analyzed extensively by Palm et al., see e.g. Palm (2013);
2. The standard *Hebbian* learning rule, see e.g. (Amari, 1977);
3. The *Hopfield* learning rule popularized by Hopfield (1982) for binary neural units and later for bipolar ones. As mentioned, here we use the Hopfield model with binary units.
4. The *Covariance* learning rule proposed in 1988 by Tsodyks and Feigelman, adding a term to the Hopfield learning rule, making independently active units developing zero weights between them (Tsodyks & Feigelman, 1988);
5. The *Presynaptic Covariance* learning rule proposed in 1997 with the intent to improve the storage capacity for correlated patterns (Minai, 1997);
6. The *BCPNN* model and learning rule derived from Bayes rule and initially proposed by Lansner & Ekeberg (1989) and later transformed to a modular version which is used today (Johansson & Lansner, 2007; Lansner & Holst, 1996).

In our tests, we evaluated these models in the non-modular architecture, which is the standard for most of them, as well as in the modular network architecture which is standard for BCPNN.

Initially, we aimed to include also the Storkey learning rule proposed in 1997 adding pre- and postsynaptic field terms to the Hopfield rule (Storkey, 1997). However, the inclusion of the presynaptic field to the synaptic weight update is local in a technical sense but violates the biologically motivated synapse locality constraint used here. Furthermore, our preliminary performance test gave worse results than most of the other rules. For these reasons, we did not include the Storkey learning rule in our comparison.

Unit output, weight update equations, and unit activation function

In this section we describe the details of the learning rules evaluated. Input and output patterns with components x_i, x_j in $[0,1]$, are sparse and random. Likewise, the neural units use (k)WTA activation giving an output in $\{0,1\}$.

The learning rules tested are all local and incremental and trained in one-shot learning. All of them can be properly formulated in terms of activity and co-activity statistics (see e.g. Minai, 1997) based on estimates of such activities, p-estimates. Synaptic update and p-estimate equations are given in Table 1 and the respective learning rule formulas in Table 2.

The field update equation for the output layer is:

$$h_j = b_j + \sum_i \pi_i w_{ij}$$

where h is the field, b is the bias, π is the presynaptic activity and w the weight.

Table 1: Synaptic state update equations. k indexes patterns.

Counter equations	p-estimate equations
$c = \sum_k 1$	-
$c_i = \sum_k x_i^{(k)}$	$p_i = \max(c_i/c, \varepsilon)$
$c_j = \sum_k x_j^{(k)}$	$p_j = \max(c_j/c, \varepsilon)$
$c_{ij} = \sum_k x_i^{(k)} x_j^{(k)}$	$p_{ij} = \max(c_{ij}/c, \varepsilon^2)$

For BCPNN $\varepsilon = 1/(1 + c)$, else $\varepsilon = 10^{-7}$

Table 2: Equations for computing bias and weight values for different learning rules

	Abbrev.	b_j	$w(x_i, y_j)$	Reference
Willshaw	WILL	-	$c_{ij} > 0$	Willshaw et al. 1969
Hebb	HEBB	-	$p_{ij} > \varepsilon$	Amari 1977
Hopfield	HOPF	-	$p_{ij} - a[p_i + p_j] + a^2, a = 1/M$	Hopfield 1982, Amari 1989
Covariance	COV	-	$p_{ij} - p_i p_j$	Tsodyks and Feigelman 1988
Presynaptic covariance	PRCOV	-	$\frac{p_{ij} - p_i p_j}{p_j}$	Minai 1997
BCPNN	BCPNN	$\log p_j$	$\log \frac{p_{ij}}{p_i p_j}$	Lansner and Ekeberg 1989

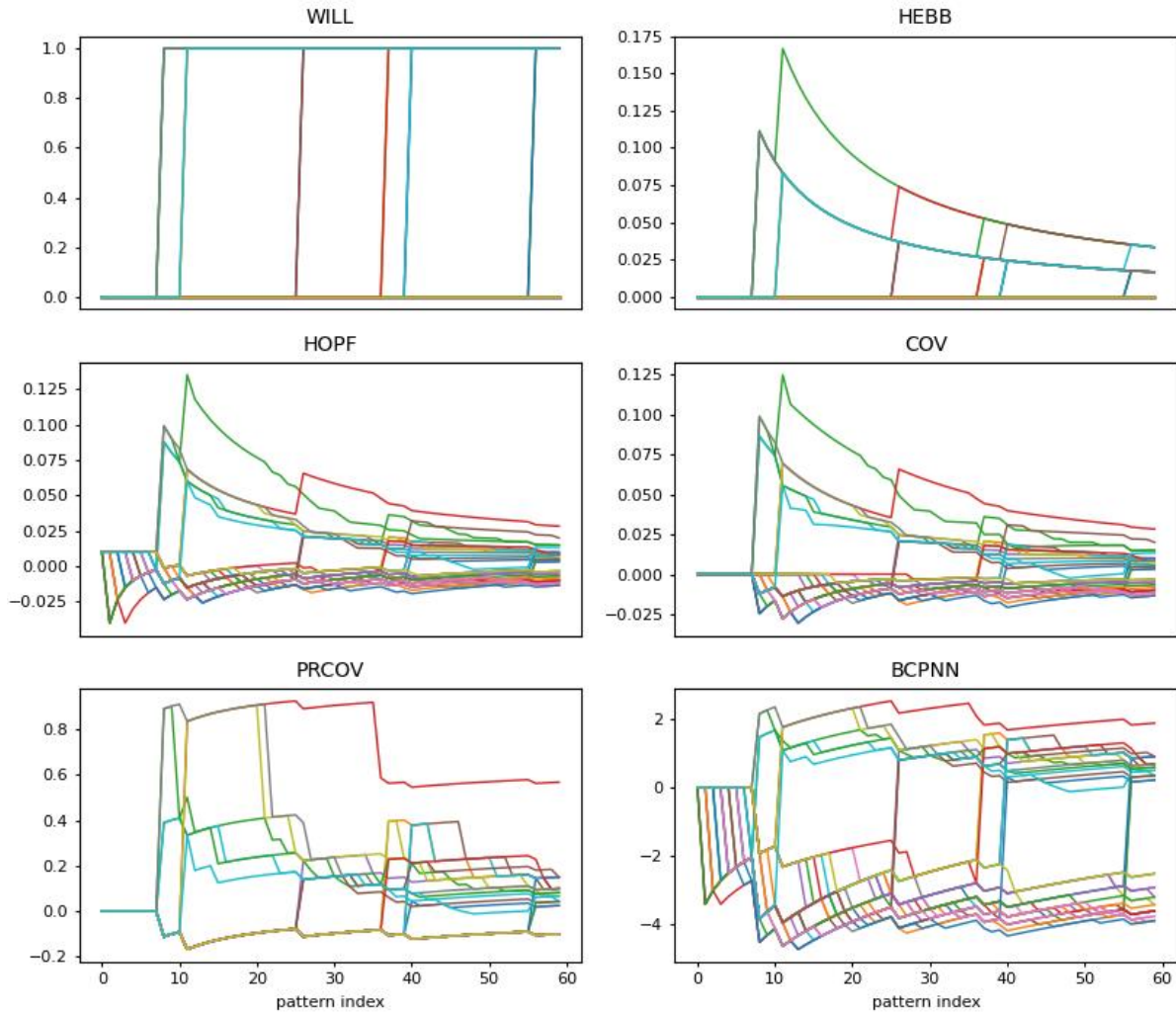


Figure 1: Weight trajectories of different learning rules. Different learning rules produce quite different weight trajectories when trained on the exact same training set with 60 patterns. Network format was 10x10 and the same set of forty weights were monitored in all cases.

Figure 1 shows the weight trajectories resulting from training networks using the different selected learning rules with the exact same sparse random patterns in same order. The overall weight magnitude ranges are quite different between the models, but the simple WTA activation makes this difference insignificant since unit activation will depend on rank of the field and not absolute values.

Experimental setup

Our comparison between the different learning rules was based on two main types of benchmark problems, i.e., storage capacity for different kinds of sparse binary patterns, and prototype extraction capability when training with distorted instances from the same kind of patterns. In both cases we measured scaling with increasing network size for non-modular and modular networks.

Pattern formats

The pattern formats used were a few variants of sparse binary patterns that could test some possibly occurring pattern forms in associative memory applications and even in the brain. We used two different binary random pattern formats for non-modular (“nrand”) and modular networks (“hrand”) respectively. We further used a “silent” format which means that a fraction of hypercolumns in the HxM networks is marked with the last unit in the hypercolumn set to 1, like a mark for “not applicable”. The same pattern format was also used to test the non-modular networks. Finally, we used correlated patterns with prefix “c” for non-modular (“cnrand”) and modular (“chrand”) networks respectively. These were generated according to a method previously presented by Minai (1997). When a hypercolumn was resampled the same constraints, whether standard or c- type, were obeyed. All pattern formats have the same number of units set.

In our study, patterns were always sparse and binary and were specified for modular “HxM” and for non-modular “KofN” networks. For the non-modular networks, to be able to compare between these two types of networks, K was chosen equal to H. A more general pattern format could have activation values in [0,1] though we here used only binary values. Three types of random patterns were investigated (Figure 2):

1. Standard binary patterns, “nrand” and “hrand”. Given the HxM format, one random unit is set active per hypercolumn and in the KofN format K active units are activated entirely randomly.
2. Binary patterns with “silent hypercolumns”. A hypercolumn is “silent” if it has the M-1’th unit set, indicating that the attribute it represents is not relevant for the current pattern, see below.
3. Correlated random modular or non-modular patterns (Minai, 1997), with the correlation parameter f_p set to 0.1 if nothing else is stated.

The motivation for the “silent hypercolumn” designation is that an earlier such pattern format considered had all hypercolumn units inactive. This was made to work properly for BCPNN and had some advantages. However, this format prevents the use of the simple (k)WTA activation function chosen in the current comparative study. We therefore opted out for it in the final benchmark suite, but decided to keep the “silent hypercolumn” concept. Now, a hypercolumn that is silent in a pattern is marked with an activation of 1 in its last unit.

The relevance of the silent pattern format (2) can be illustrated if we consider a database of different kinds of objects, characterized by a set of attributes, e.g. weight, length, colour, number-of-wheels, top-speed, number-of-legs, inkubation time, etc. each discrete coded by one hypercolumn. Since for a specific object, only a fraction of all attributes would be relevant, the remaining ones would be “silent”. In a complex database, containing a wide variety of object, the fraction of such irrelevant attributes could be quite large.

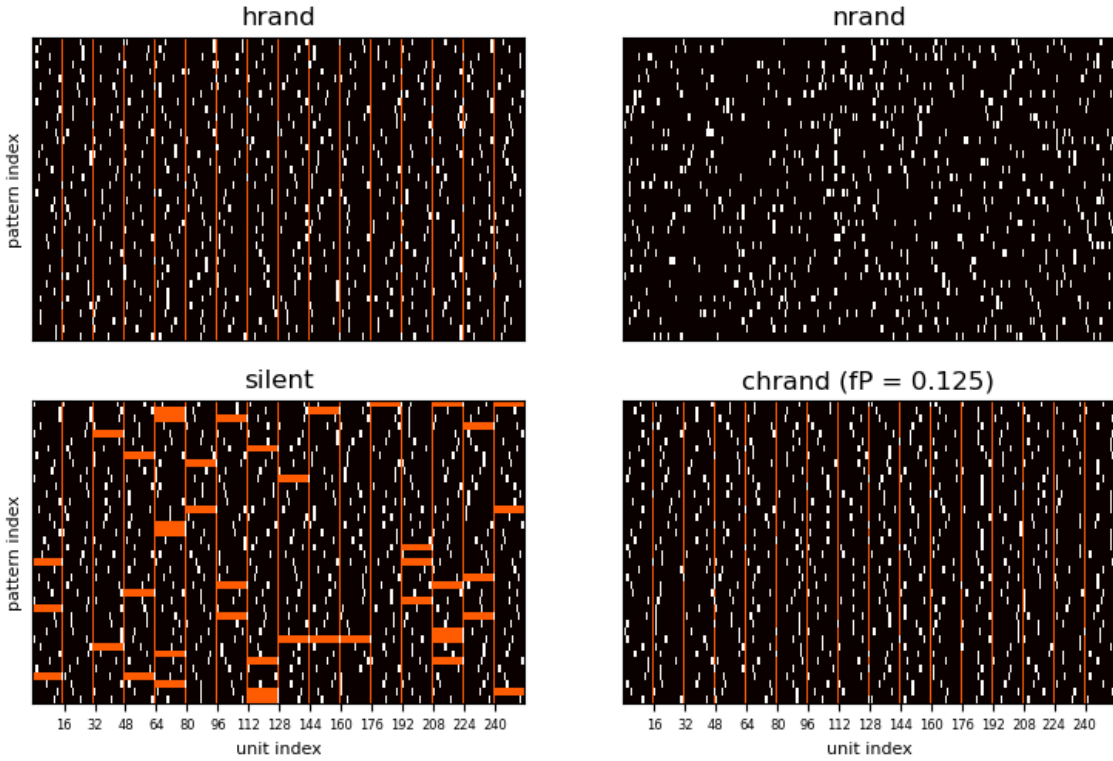


Figure 2: Four different pattern types used. Sets of forty 16x16 patterns are shown. The “silent hypercolumns” (marked orange) have their last unit set to 1. The “cnrand” type of patterns are not shown. Vertical orange lines mark the last unit in hypercolumns.

When nothing else is stated, the number of silent HCs in patterns was scaled as $h_{\text{sil}} = 0.25 * H$. Since h_{sil} is integer, for non-integer values of h_{sil} the $\text{floor}(h_{\text{sil}})$ and $\text{ceil}(h_{\text{sil}})$ were mixed proportionally to the fraction part of the distortion value to achieve a proper mean distortion.

Pattern storage capacity

To measure storage capacity, the number of stored patterns was increased until the exact recall fraction from a test set of distorted test patterns fell below a specified threshold, e.g. 90%. Since the process is probabilistic a stochastic bisection method was used to estimate the crossing (Supplement S1).

Figure 3 exemplifies how the fraction of correct recall from distorted patterns falls with the number of random patterns stored in a trained modular network. The result is qualitatively the same for a trained non-modular network. As seen from the error bars in the top row, the standard deviation is quite high among different networks storing the same number of patterns. It is clear that learning rules can store different number of patterns, lowest for the HEBB and highest for the BCPNN learning rule, with the others in between. The type of binary pattern also affects network performance significantly.

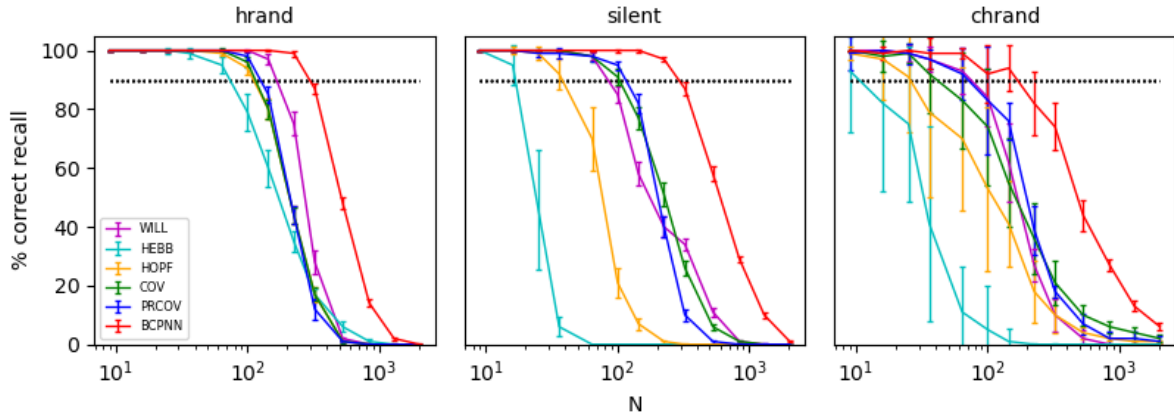


Figure 3: Recall fraction of a modular network ($H = 16$, $M = 16$) depending on pattern type and number of patterns stored for different learning rules. The network was trained with increasing number of patterns while recall fraction fell to low values. The dotted line marks 90% recall fraction. Two hypercolumns were resampled in test patterns and error bars here show standard deviation. The number of test repeats per data point was 20.

The pattern distortion for creating test patterns and instances from pattern prototypes were done by resampling a specified fraction of active units in a pattern. Training constituted one pass over the training set, i.e. one-shot learning. Input patterns were activated and clamped whereafter the learning machinery was applied. During testing, the task of the network was to reconstruct the correct pattern from distorted test patterns with a specified number of hypercolumns resampled. We required perfect reconstruction for correct recall. Max number of iterations were set to ten, but fewer was most often required to reach a stable state. It was monitored if last and next to last activity state differed. This happened in much less than 1 % of runs and did not significantly affect reported recall performance.

The number of binary patterns possible to store in a network is, in fact, not a good measure of its storage capacity. For instance, that number is highly dependent on the activity density of the patterns, or more precisely, the information content of each pattern. Patterns with few active units contain less information and can be stored reliably in higher numbers than more dense patterns. As is discussed below about fitting the storage capacity relation, a more stable measure in this context is the number of bits of information stored in the network relative to the number of free parameters, i.e. the number of weights (or half of that for a symmetric weight matrix).

Prototype extraction and recall

For prototype extraction, several random prototype patterns were generated and from each of them a number of distorted instances were generated by resampling as above. Such distorted patterns were used both for training and testing. The task of the network was to recall the prototype pattern from a distorted version of it (Figure 4). As can be seen from the bottom row, the network was able to reconstruct one of the prototypes almost perfectly when given eight or more instances for training. The same prototype extraction happened for the nine other prototypes. Notably, the calculation of the mean in the middle row was done given information of from which prototype a pattern instance was generated. This information was not provided for the network, which therefore solved a harder problem.

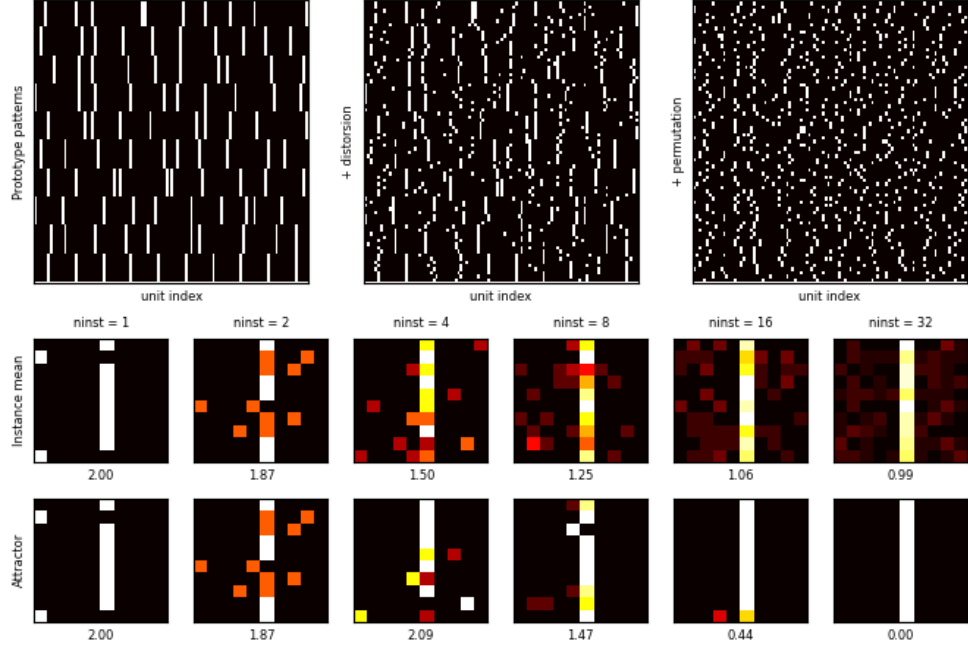


Figure 4: Prototype extraction from different number of instances. Top, left: 10 random 10x10 prototype patterns, one per row. Top, middle: 32 training instances from each of the 10 prototypes. Each instance was resampled in 3 randomly selected hypercolumns. Top, right: The training instances in randomly permuted order forming the final training set. The panels in the second row show means of the ‘ninst’ instances for each prototype pattern. The bottom row shows the prototype pattern extracted by a BCPNN trained with instance patterns and tested with previously unseen such patterns. The number below each panel in the two lower rows gives the average distance between the test and prototype pattern for the last prototype displaying in 2D as a bar (last row in Top, left panel).

Fitting functions for storage capacity scaling

One way to derive a fitting function for the pattern storage capacity given the sparse distributed random binary patterns used in this work is to calculate the number of entries in the connection weight matrix of the network, N_w , and divide it by the information stored per pattern, I_p . Then the number of patterns P possible to store can be expected to scale as N_w/I_p or for a symmetric W as $N_w/2/I_p$, where $N_w/2$ is the number of free weights (parameters) in the recurrent network.

The total information contained in the free parameters is calculated as

$$I_w = \frac{N^2}{2} I_w \quad (1)$$

where I_w represents the number of bits stored per weight. The number of bits per pattern stored is calculated as

$$I_p = \log_2 \binom{N}{K} \quad (2)$$

for the non-modular network and as

$$I_p = H \log_2 M \quad (3)$$

for the modular network.

From these relations P can be calculated as I_w/I_p :

$$P = \frac{N^2}{2 \log_2 \binom{N}{K}} I_w \quad (4)$$

For the non-modular networks and

$$P = \frac{N^2}{2H \log_2 M} I_w \quad (5)$$

for the modular networks, with the only free variable being I_w in both cases.

The relation derived indicates that the amount of information stored in the network scales with the number of free parameters, i.e. the number of weights in the networks.

Results

In this section we give results on storage capacity and prototype extraction for the six different learning rules and for different network architectures and pattern types. Results are mainly derived in the form of how the number of correctly recalled patterns/prototypes scale with network size. We further check the fit between theoretical estimates given above and experimental results.

Storage capacity scaling

In this section we give results from training networks with increasing number of stored patterns of the different types and testing them with regard to fraction of patterns recalled when stimulated with distorted versions of the trained patterns. That allows us to characterize how the storage capacity increases with network size and how this depends on the learning rule.

Figure 5 shows how the pattern storage capacity measured at the crossing with the 90 % exact recall limit depends of network size for non-modular (upper panels) and modular (lower panes) networks. It is evident that the storage capacity for different random pattern types varies with learning rules and that some of these are very sensitive to the silent and correlated pattern types. Notably, the HEBB and HOPF and also the WILL learning rule with binary weights fell back quite dramatically for the silent and correlated pattern formats. The COV and PRCOV learning rules were quite robust but at a modest storage capacity. The BCPNN learning rule benefits from the silent pattern format and is further quite resilient to correlations among patterns. Notably, BCPNN demonstrates highest capacity with a significant margin for all cases tested here. The picture is quite similar for the non-modular vs modular network architectures with the same ranking of the learning rules, though the number of patterns possible to store is somewhat higher for the modular case. As shown below, this is explained by the slightly lower amount of information contained in each modular pattern.

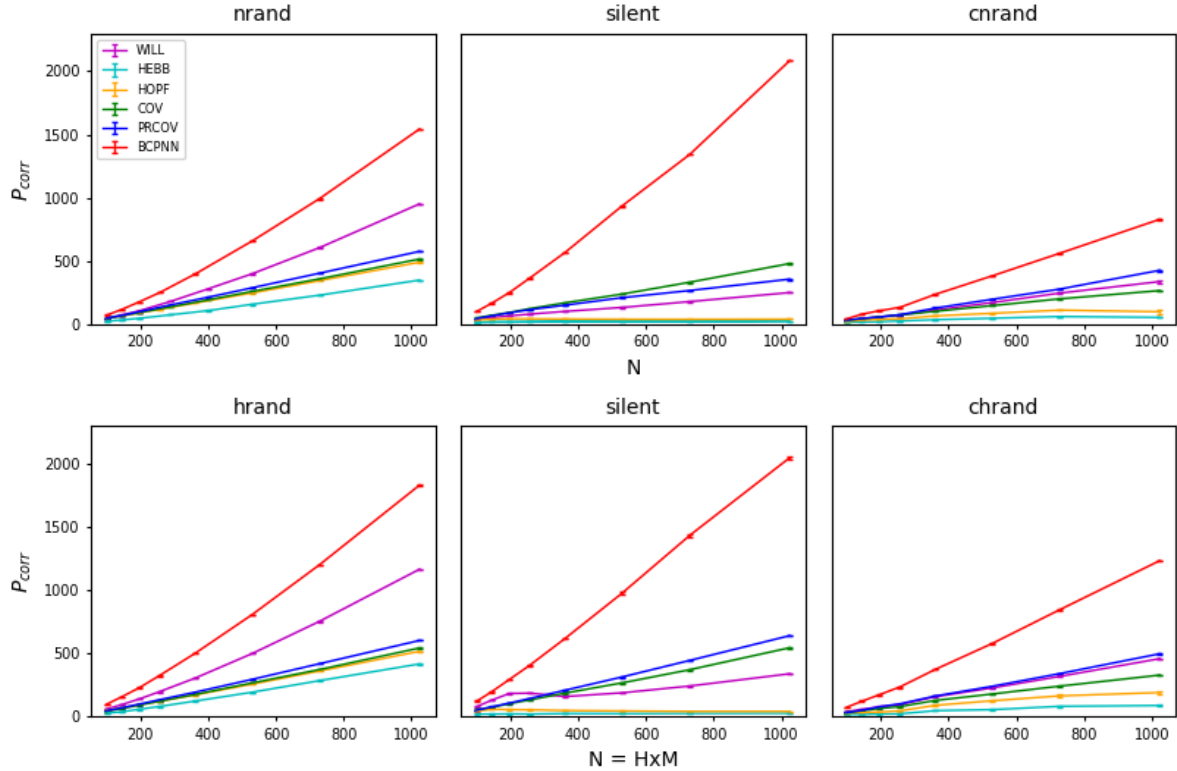


Figure 5. Storage capacity of non-modular and modular networks depending on type of pattern type and learning rule. Performance measured as maximum number of patterns (P_{corr}) that allows for exact recall fraction above 90%. Upper and lower panels show data for non-modular and modular networks respectively. Each data point is the mean and standard deviation of 5 runs. In the test patterns, 10 % of the units were resampled. For the silent pattern format the fraction of silent hypercolumns was 25% and for the correlated pattern type the correlation parameter was 0.1. Legend in upper row left panel holds for all panels.

Fitting the theoretical storage capacity relations

The theoretical relations given in eqns 4 and 5 were used to fit the empirical results derived above, for the standard random binary pattern types (hrand, nrand). The relations $H = K = \sqrt{N}$, used for the respective network configuration were also imposed, whereby I_w remained the only free parameter. As shown in Figure 6, the fit is quite good. From this fit we got the values of I_w , the estimated information stored per free weight, for each learning rule and network type, shown in Table 3. As can be seen, the numbers are quite similar for the two network types, though the actual number of patterns possible to store are significantly different.

	HEBB	HOPF	COV	PRCOV	WILL	BCPNN
Non-modular	0.14	0.20	0.22	0.24	0.41	0.60
Modular	0.13	0.17	0.18	0.20	0.37	0.57

Table 3: Estimated information in bits stored per weight. Data refer to the h/nrand pattern types.

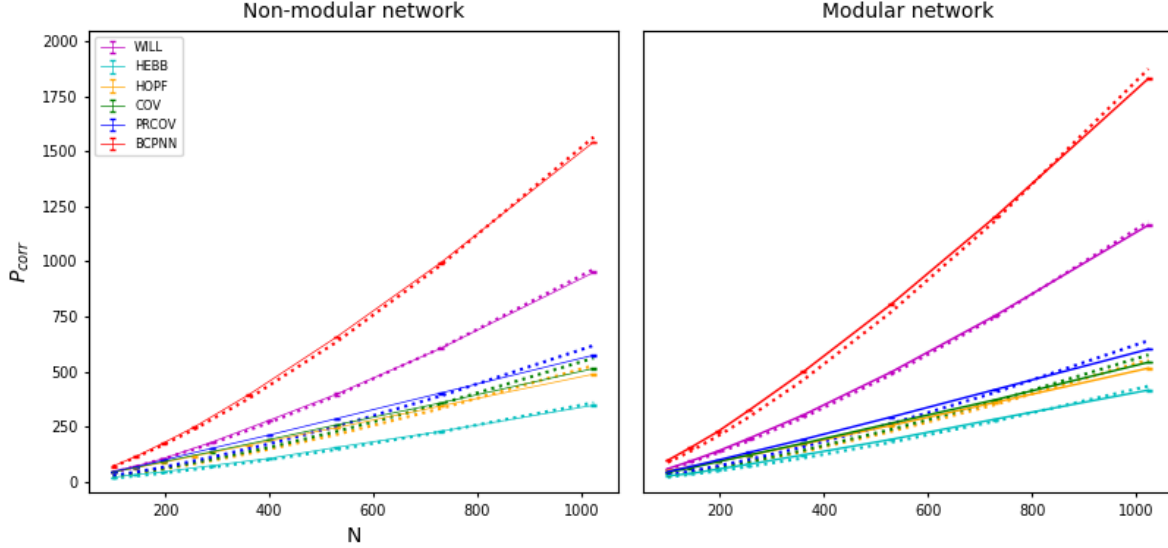


Figure 6: Estimating bits per connection. Storage capacity scaling curves were fitted (dotted lines) using Eqns. 4 and 5 above. The I_w values were according to Table 3.

Further exploration of fraction of distorted and silent hypercolumns

We explored further the performance scaling of the different learning rules while changing the amount of test sample distortion (BCPNN learning rule) and fraction of silent hypercolumns in the patterns stored (Figure 7). The dependency of measured storage capacity on different levels of distorted (resampled) hypercolumns was investigated only for BCPNN as it demonstrated the highest bits per weight value. As shown in Figure 7 left panel, the capacity increased gradually with less distortion ending with a value of 0.78 bits per weight. The stability of the non-distorted pattern was very high, even in the presence of noise, so extrapolation to zero was not possible. Regarding the dependency of fraction of silent hypercolumns (Figure 7, right panel), the HOPF, HEBB, COV, and PRCOV rules failed to store more patterns with higher numbers. The WILL rule had problems at mid-range, but recovered for high fractions of silent hypercolumns. The BCPNN rule performed well over the entire range, showing high flexibility and good scaling properties. An explanation for these quite mixed and non-monotonous dependencies remains to be derived. Notably, for the BCPNN rule, earlier studies (unpubl.) have shown that it is also possible to omit the marking of hypercolumns with an active “na” unit thus making the hypercolumns truly silent and the activity patterns sparse. Here, however, with the use of the WTA activation function we could not further investigate this setup.

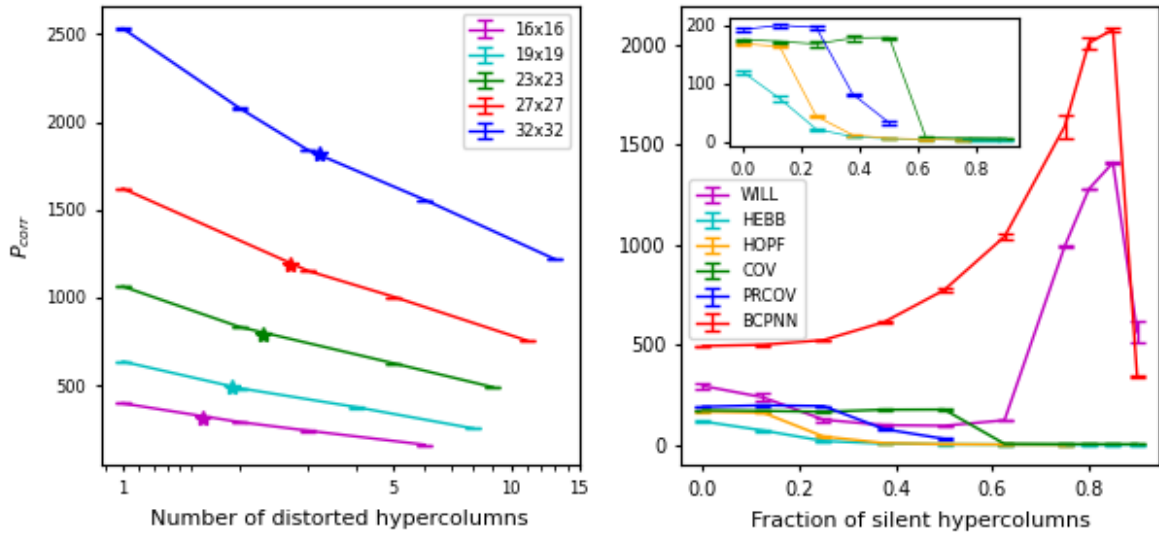


Figure 7: Left panel: Storage capacity at different amount of pattern distortion shown for different size networks using the BCPNN learning rule. Standard deviation was calculated from three repetitions. The 10% level distortion is shown with a * for each network size. Abscissa is logarithmic. **Right panel: Recall at high fraction of silent hypercolumns.** A 19x19 network using the different learning rules was trained with patterns with increasing fraction of silent hypercolumns. 10% of the active hypercolumns were distorted in the test patterns. Average and standard deviation of three runs is shown. The inset magnifies the low range of capacities.

Prototype extraction

The prototype extraction capabilities of different network architectures and learning rules were evaluated in a similar way as storage capacity scaling. The main difference was that instead of training with a number of (prototype) patterns as such, training was done with instances generated by distortion from a set of training patterns (the prototypes). The networks were tested for ability to reconstruct the generating prototype from a new distorted test pattern.

In order to give an impression of some details of prototype extraction, Figure 8 shows how the fraction of correctly recalled prototype patterns depended on number of instances (ninst) for a fixed size network ($H = 16$, $M = 16$) using the BCPNN learning rule. As can be seen, performance is steadily increasing with a higher number of instances and only ten instances are required to approach highest performance. The number of prototypes possible to extract and store is, however, quite a bit lower than if the prototypes themselves are given during training (Figure 8, dashed curve). Another feature of this setup is the bimodal performance with increasing number of prototypes at intermediate number of instances. The reason for this behavior remains to be further investigated, but could partly be explained by that networks with low pattern load and number of instances recall instances instead of prototypes, which is then recorded as an error.

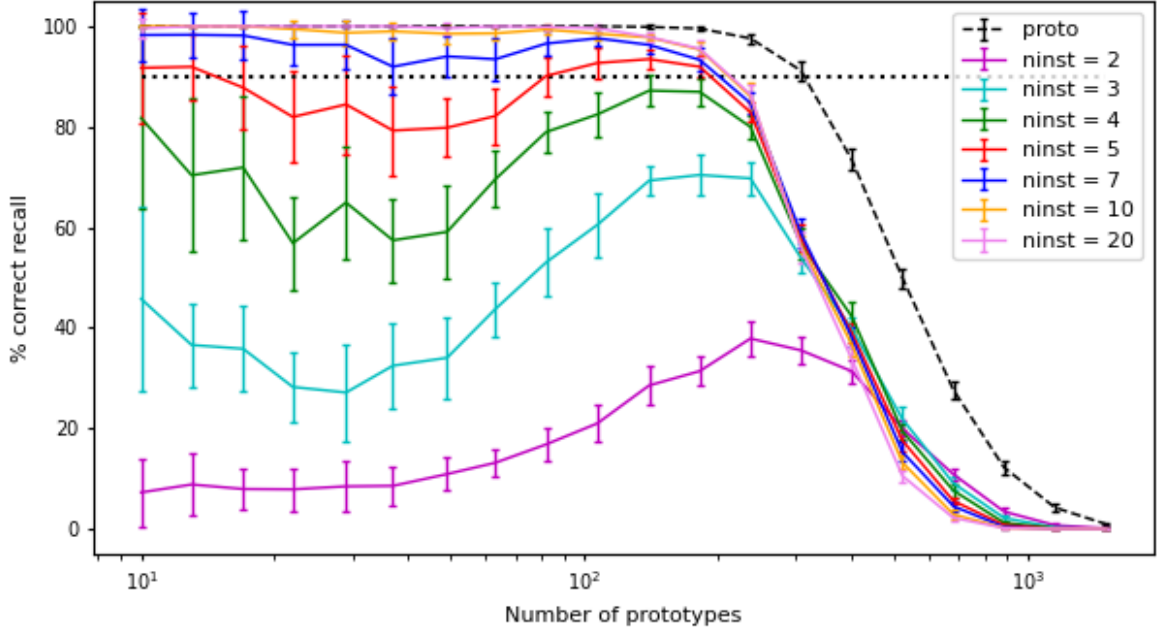


Figure 8: Fraction of correct recall dependence of number of prototypes and training instances. Storage capacity of a modular 16x16 BCPNN network when trained with variable number of prototype patterns and number of instances generated from those. Two hypercolumns were resampled in training and test instances. The number of training instances is color coded according to the legend. The dashed black line shows performance when only the prototype patterns themselves were stored. Error bars show standard deviation from 20 repetitions.

Figure 9 shows the storage capacity scaling with network size for the six learning rules and six pattern types. As can be seen, the storage capacity was overall lower than for random patterns and the spread of performance between the rules was substantial. It is not unexpected that the WILL learning rule failed entirely, likely because it has binary weights. Moreover, the performance of the HEBB and HOPF learning rules was generally very poor for silent and correlated pattern types, especially for non-modular networks. The covariance type learning rules were quite robust but showed relatively low performance. Again, BCPNN showed top performance except in the case with non-modular network configuration and correlated pattern type where it failed even more severely than the covariance learning rules. However, we found that this case could easily be rescued by some parameter tuning which, however, was not considered relevant for this comparative study.

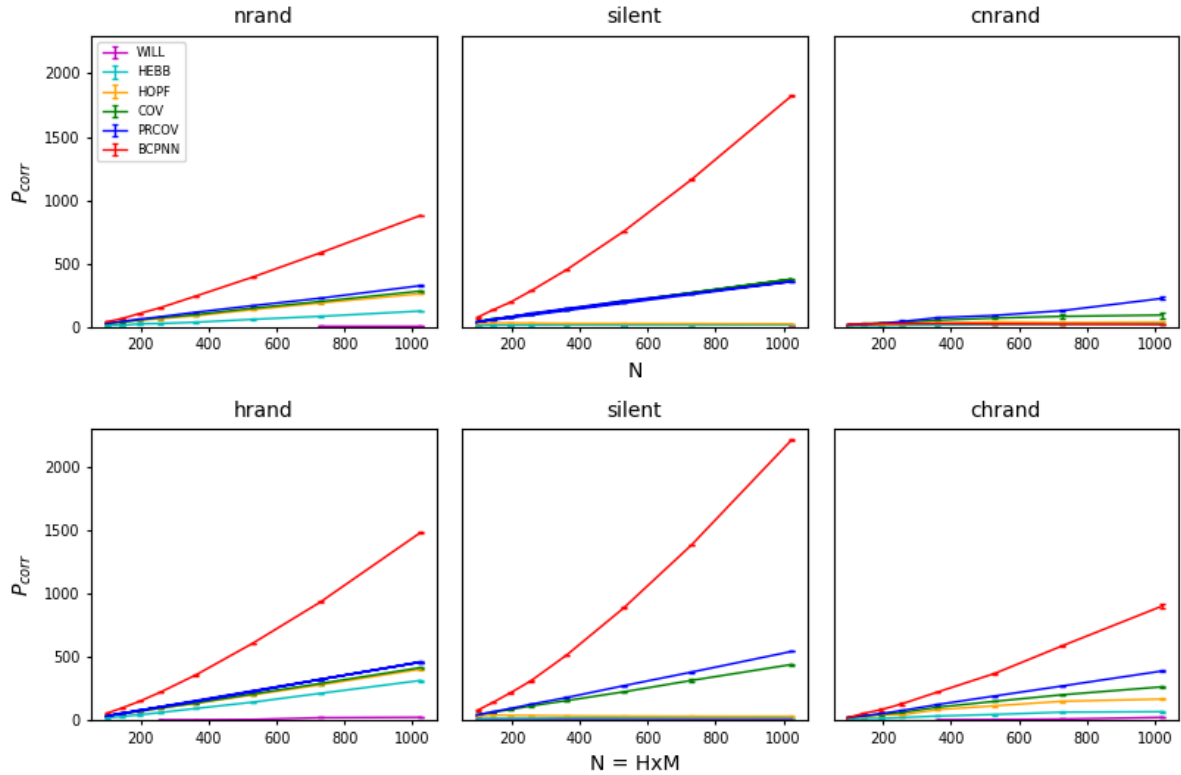


Figure 9: Prototype extraction storage capacity. Performance measured as maximal number of prototypes allowing exact prototype recall above 90% depending on type of prototype pattern and learning rule. Upper row refers to non-modular networks, lower row to modular networks. The number of training instances was 10 and 10% of hypercolumns were resampled in both training and test instances. For the silent pattern format, the fraction of silent columns was 25% and for the correlated pattern format the correlation parameter was 0.1. Legend in upper row left panel holds for all panels.

Discussion

In this work we have compared quantitatively by means of extensive computer simulations six different learning rules with regard to associative memory pattern processing capabilities in terms of pattern storage capacity and prototype extraction. We used three different sparse random pattern types with non-modular and modular network architectures. Generally, the difference between non-modular and modular architectures were marginal. They stored the same amount of information though the non-modular one stored somewhat fewer patterns with higher information content per pattern. Pattern type, however, had a significant impact on performance and silent and correlated random pattern types challenged the learning rules, typically leading to reduced and sometimes disappearing performance.

The overall outcome for pattern storage capacity scaling was that the BCPNN learning rule is superior with quite a large margin, to the other learning rules (Figures 5 and 7). The second best one is the WILL learning rule and worst is the HEBB rule. It is noteworthy that the BCPNN rule is still best even for correlated patterns, with the PRCOV rule second best, despite that the latter was developed to optimize performance on correlated patterns. The HOPF rule shows a slightly better performance than HEBB. These results differ from many earlier theoretically derived and reported pattern storage capacities, likely explained by the fact that the testing

setup here is with finitely sparse random binary patterns different from the often used dense or infinitely sparse patterns and bipolar pattern formats.

For prototype extraction, the picture was somewhat different. Firstly, the task was generally quite a bit harder than storage of individual patterns. The WILL rule failed entirely which is expected due to its binary weight matrix. So even though increasing the number of bits to 32 as for the other learning rules does not increase storage capacity scaling *per se*, it supports prototype extraction capacity and robustness. Even for the non-binary weight matrixes, precision could likely be lowered significantly, though this is not investigated further here (Vogginger et al., 2015)(Vogginger et al., 2015)). The HEBB and HOPF rules managed with standard binary patterns but otherwise fell back to chance performance. Regarding correlated patterns, the correlation parameter of 0.1 did affect prototype extraction performance of all rules significantly. In particular, the BCPNN rule while superior in other cases was severely affected for the non-modular network architecture, whereas the PRCOV performed best and the COV rule showed stable performance. These two learning rules thus displayed a high robustness over all cases, but at a relatively low level of performance.

	Storage capacity scaling						Prototype extraction						Overall mean	
	Non-modular			Modular			Non-modular			Modular				
	nrand	silent	crand	hrand	silent	chrand	nrand	silent	crand	hrand	silent	chrand		
WILL	950	248	335	1165	337	457	3	13	0	23	3	22	296	
HEBB	346	13	51	415	25	86	124	14	23	314	18	67	125	
HOPF	488	37	96	515	40	189	260	22	37	403	31	167	190	
COV	513	478	264	542	543	327	281	205	92	415	440	264	364	
PRCOV	574	354	424	601	639	496	324	193	224	461	543	389	435	
BCPNN	1543	2048	828	1831	2048	1233	879	1824	17	1483	2214	903	1404	

Table 3: Summary of learning rule performance over all conditions. The table shows the number of patterns stored with 90% recall criterion for $N = 1024$ size networks. The average numbers are given in the framed last column.

The results from all benchmark runs are summarized in Table 3. It can be seen that the overall performance of BCPNN is more than 3x that of the runner up, which is PRCOV. Part of an explanation might be that BCPNN was derived from naïve Bayes formalism for probabilistic inference and operates in log space thus combining evidence multiplicatively rather than additively, in contrast to all the other learning rules. For random patterns, the underlying independence assumption for naïve Bayes is likely to hold quite well.

Regarding parameter sensitivity there were not many hyper parameters in this experimental setup. Yet, one structural parameter we fixed in our investigation is the size of the hypercolumns in the modular network, at \sqrt{N} , making the size and number of such hyper- and minicolumns identical. This partitioning scheme was suggested by Braitenberg (1978) on the basis of cortical architecture, though with different types of modules in mind. This scheme works nicely for small to medium scale simulations of the type used here but does not scale to biological cortex sizes. The estimated number of minicolumns per hypercolumn in mammalian cortex is on the order of hundreds, so the number of hypercolumns would scale to much larger values. It is unclear to what extent our simple scaling estimates hold for such networks. And

uncertainty about the actual activity density in higher order cortex is a further complication. Possibly, the number of silent hypercolumns is quite high, thus resulting in more sparse patterns and a higher pattern storage capacity (Figure 7, right panel). Another important parameter in a brain-scale networks is the density of connectivity between minicolumns, which would come out higher than that between neurons in the neocortex, but still far below the 100 % used in this study. With a maintained bits per weight such dilution of connectivity would proportionally reduce the storage capacities seen in this study.

Future Works

The procedure used here for benchmarking of associative memory performance could be applied to many other learning rules than those included in this study. It remains also to extend the parameter ranges tested here, like HxM configurations, scaling to larger network sizes, etc.

Another interesting development is to investigate the impact of using spiking neural units instead of graded output ones. Eventually, this can be further developed with more biophysically detailed neuron models and realistic neural circuitry leading to a better understanding of the associative memory capacity of neural networks of different regions of cortex (Cutsuridis, 2019).

More importantly the set of associative pattern processing functions tested should be extended to quantitative assessment of more advanced capabilities like temporal sequence learning and recall and integration of multi-layer architectures and feature extracting structural plasticity into these NAM:s (see for example (Knoblauch & Sommer, 2016; Krotov & Hopfield, 2021; N. Ravichandran et al., 2020). The use of similar learning rules in spiking neural network models of the cortex brings closer brain-like AI and brain models of memory and cognitive processing (Chrysantidis et al., 2022; Fiebig et al., 2020; Ravichandran et al., 2023; Tully et al., 2016).

Furthermore, going beyond the mere one-shot infinite-term memory scenarios studied here is important, i.e. to test learning and memory at different timescales, from repeated storing of stimuli etc. This could address memory formation over longer timescales and the ability to combine associative memories operating on different timescales for e.g. short-term, working memory to long-term memory, including systems consolidation (Fiebig & Lansner, 2014).

By developing our brain-like NAM models in these directions we hope to improve our understanding of cortical associative memory and also to promote these so far grossly neglected architectures and learning rules as essential components in future AI and machine learning systems.

Acknowledgements.

We would like to thank the Swedish Research Council (VR) grants: 2018-05360 and 2016-05871, Digital Futures and Swedish e-science Research Center (SeRC) for support.

References

Amari, S. (1977). Neural Theory of Association and Concept-Formation. *Biol. Cybernetics*, *26*, 175–185.

Amari, S. (1989). Characteristics of sparsely encoded associative memory. *Neural Networks*, *5*(451–457).

Anderson, J. A., Silverstein, J. W., Ritz, S. A., & Jones, R. S. (1977). Distinctive Features, Categorical Perception, and Probability Learning: Some Applications of a Neural Model. *Psychological Review*, *84*, 414–451.

Braitenberg, V. (1978). Cortical architectonics: general and areal. In M. A. B. Brazier & H. Petsche (Eds.), *Architectonics of the Cerebral Cortex* (pp. 443–465). Raven Press.

Burgess, N., Shapiro, J., & Moore, M. (1991). Neural network models of list learning. *Network: Computation in Neural Systems*, *2*, 399–422.

Carandini, M., Heeger, D. J., & Movshon, J. A. (1997). Linearity and Normalization in Simple Cells of the Macaque Primary Visual Cortex. *The Journal of Neuroscience*, *17*, 8621–8644.

Chrysantidis, N., Florian Fiebig, F., Anders Lansner, A., & Herman, P. (2022). Traces of semantization - from episodic to semantic memory in a spiking cortical network model. *ENeuro*, *9*(4). <https://doi.org/doi.org/10.1523/ENEURO.0062-22.2022>

Cutsuridis, V. (2019). Improving the Recall Performance of a Brain Mimetic Microcircuit Model. *Cognitive Computation*, *11*, 644–655.

Egorov, A. v., Hamam, B. N., Fransén, E., Hasselmo, M. E., & Alonso, A. A. (2002). Graded persistent activity in entorhinal cortex neurons. *Nature*, *420*, 173–178.

Fernandino, L., Tong, J.-Q., Conant, L. L., Humphries, C. J., & Binder, J. R. (2022). Decoding the information structure underlying the neural representation of concepts. *PNAS*. <https://doi.org/10.1073/pnas.2108091119/-/DCSupplemental>

Fiebig, F., Herman, P., & Lansner, A. (2020). An Indexing Theory for Working memory based on Fast Hebbian Plasticity. *ENeuro*, *7*(2), 1–22. <https://doi.org/https://doi.org/10.1523/ENEURO.0374-19.2020>

Fiebig, F., & Lansner, A. (2014). Memory consolidation from seconds to weeks: a three-stage neural network model with autonomous reinstatement dynamics. *Frontiers in Computational Neuroscience*, *8*, 1–17. <https://doi.org/10.3389/fncom.2014.00064>

Fiebig, F., & Lansner, A. (2017). A spiking working memory model based on Hebbian short-term potentiation. *J Neurosci*, *37*(1), 83–96. <https://doi.org/DOI: http://dx.doi.org/10.1523/JNEUROSCI.1989-16.2016>

Fiorelli, E., Lesanovsky, I., & Müller, M. (2022). Phase diagram of quantum generalized Potts-Hopfield neural networks. *New Journal of Physics*, *24*(3), 033012. <https://doi.org/10.1088/1367-2630/ac5490>

Gabor, D. (1968). Holographic Model of Temporal Recall. *Nature*, *217*, 584.

Gerstner, W., Kistler, W. M., Naud, R., & Paninski, L. (2014). Chapter 19.2 Models of Hebbian learning. In *Neuronal Dynamics: From single neurons to networks and models of cognition*. Cambridge University Press.

Hebb, D. O. (1949). *The Organization of Behavior: A neuropsychological theory*. John Wiley Inc.

Hopfield, J. J. (1982). Neural networks and physical systems with emergent collective computational abilities. *Proceedings of the National Academy of Sciences of the United States of America*. <https://doi.org/10.1073/pnas.79.8.2554>

Johansson, C., & Lansner, A. (2007). Towards cortex sized artificial neural systems. *Neural Networks*, 20(1). <https://doi.org/10.1016/j.neunet.2006.05.029>

Kanter, I. (1988). Potts-glass models of neural networks. *Physical Rev A*, 37(7), 2739–2742.

Knoblauch, A., & Palm, G. (2020). Iterative retrieval and block coding in autoassociative and heteroassociative memory. *Neural Computation*, 32(1), 205–260. https://doi.org/10.1162/neco_a_01247

Knoblauch, A., & Sommer, F. T. (2016). Structural plasticity, effectual connectivity, and memory in cortex. *Frontiers in Neuroanatomy*, 10(JUNE). <https://doi.org/10.3389/fnana.2016.00063>

Krotov, D., & Hopfield, J. J. (2019). Unsupervised learning by competing hidden units. *Proceedings of the National Academy of Sciences*, 116(16), 7723–7731. <https://doi.org/10.1073/PNAS.1820458116>

Krotov, D., & Hopfield, J. J. (2021). Large Associative Memory Problem in Neurobiology and Machine Learning. *ICLR 2021 Poster*, 1–12.

Lansner, A. (1985). Pattern Processing in a Multi-layer Associative Net. *4th Scandinavian Conference on Image Analysis*, 753–760.

Lansner, A. (1986). *Investigations into the Pattern Processing Capabilities of Associative Nets*. Royal Institute of Technology, Stockholm, Sweden, Dept. of Numerical Analysis and Computing Science.

Lansner, A., & Ekeberg, Ö. (1987). An associative network solving the “4-Bit ADDER problem.” In M. Caudill & C. Butler (Eds.), *IEEE First International Conference on Neural Networks* (pp. II–549).

Lansner, A., & Ekeberg, Ö. (1989). A one-layer feedback artificial neural network with a Bayesian learning rule. *Int. J. Neural Systems*, 1, 77–87.

Lansner, A., & Holst, A. (1996). A higher order Bayesian neural network with spiking units. *Int. J. Neural Systems*, 7(2), 115–128.

Lansner, A., Marklund, P., Sikström, S., & Nilsson, L. (2013). Reactivation in Working Memory: An Attractor Network Model of Free Recall. *PloS One*, 8(8), e73776. <https://doi.org/10.1371/journal.pone.0073776>

Longuet-Higgins, H. C. (1968). Holographic Model of Temporal Recall. *Nature*, 217, 104.

Lundqvist, M., Compte, A., & Lansner, A. (2010a). Bistable, Irregular Firing and Population Oscillations in a Modular Attractor Memory Network. *PLoS Comput Biol*, 6(6), 1–12. <https://doi.org/doi:10.1371/journal.pcbi.1000803>

Lundqvist, M., Compte, A., & Lansner, A. (2010b). Bistable, irregular firing and population oscillations in a modular attractor memory network. *PLoS Comput Biol.*, 6(6).

Lundqvist, M., Herman, P., & Lansner, A. (2011). Theta and gamma power increases and alpha/beta power decreases with memory load in an attractor network model. *Journal of Cognitive Neuroscience*, 23(10). https://doi.org/10.1162/jocn_a_00029

Mari, C. F., & Treves, A. (1998). Modeling neocortical areas with a modular neural network. In *BioSystems* (Vol. 48).

Marr, D. (1971). Simple memory: a theory for archicortex. *Phil. Trans. Royal Soc. London*, 262, 23–81.

Meyniel, F., Sigman, M., & Mainen, Z. F. (2015). Confidence as Bayesian Probability: From Neural Origins to Behavior. In *Neuron* (Vol. 88, Issue 1, pp. 78–92). Cell Press. <https://doi.org/10.1016/j.neuron.2015.09.039>

Minai, A. (1997). Covariance Learning of Correlated Patterns in Competitive Networks. *Neural Comput*, 9, 667–681. <http://direct.mit.edu/neco/article-pdf/9/3/667/813651/neco.1997.9.3.667.pdf>

Naim, M., Boboева, V., Kang, C. J., & Treves, A. (2018). Reducing a cortical network to a Potts model yields storage capacity estimates. *Journal of Statistical Mechanics: Theory and Experiment*, 2018(4). <https://doi.org/10.1088/1742-5468/aab683>

Nakano, K. (1972). Associatron - A model of associative memory. *IEEE Trans of Systems, Man, and Cybernetics*, 2, 380–388.

Palm, G. (1980). On Associative Memory. *Biol. Cybernetics*, 36, 19–31.

Palm, G. (2013). Neural associative memories and sparse coding. *Neural Networks*, 37, 165–171. <https://doi.org/10.1016/j.neunet.2012.08.013>

Ravichandran, N., Lansner, A., & Herman, P. (2020). Learning representations in Bayesian Confidence Propagation neural networks. *2020 International Joint Conference on Neural Networks (IJCNN)*, 1–7. <https://doi.org/10.1109/IJCNN48605.2020.9207061>

Ravichandran, N., Lansner, A., & Herman, P. (2023). *Spiking neural networks with Hebbian plasticity for unsupervised representation learning*. <https://doi.org/10.48550/arXiv.2305.03866>

Rochester, N., Holland, J. H., Haibt, L. H., & Duda, W. L. (1956). Tests on a cell assembly theory of the action of the brain, using a large digital computer. *IRE Trans. Information Theory*, IT-2, 80–93.

Ross, M., Chartier, S., & Hélie, S. (2017). The neurodynamics of categorization: Critical challenges and proposed solutions. In *Handbook of Categorization in Cognitive Science* (pp. 1053–1076). Elsevier. <https://doi.org/10.1016/B978-0-08-101107-2.00042-7>

Schwenker, F., Sommer, F. T., & Palm, G. (1996). Iterative Retrieval of Sparsely Coded Associative Memory Patterns. In *Neural Networks* (Vol. 9, Issue 3).

Stuchlik, A. (2014). Dynamic learning and memory, synaptic plasticity and neurogenesis: An update. In *Frontiers in Behavioral Neuroscience* (Vol. 8, Issue APR). Frontiers Research Foundation. <https://doi.org/10.3389/fnbeh.2014.00106>

Tamosiunaite, M., Kulvicius, T., & Wörgötter, F. (2022). *Bootstrapping Concept Formation in Small Neural Networks*.

Tsodyks, M. v., & Feigelman, M. v. (1988). Enhanced Storage Capacity in Neural Networks with Low Level of Activity. *Europhys Lett*, 6(2), 101–105.

Tully, P. J., Lindén, H., Hennig, M. H., & Lansner, A. (2016). Spike-Based Bayesian-Hebbian Learning of Temporal Sequences. *PLoS Computational Biology*, 12(5). <https://doi.org/10.1371/journal.pcbi.1004954>

Vogginger, B., Schüffny, R., Lansner, A., Cederström, L., Partzsch, J., & Höppner, S. (2015). Reducing the computational footprint for real-time BCPNN learning. *Frontiers in Neuroscience: Neuromorphic Engineering*, 9(January), 1–16. <https://doi.org/10.3389/fnins.2015.00002>

Willshaw, D. J., Buneman, O. P., & Longuet-Higgins, H. C. (1969). Non-holographic associative memory. *Nature*, 222, 960–962.

S1 – Stochastic bisection method for estimating the number of stored patterns giving 90% correct recall

The pseudo-code used for efficient estimate of the crossing with the 90% level is given below. P0 was estimated from the theoretical max capacity with random binary patterns. The estimated value and spread is mean and standard deviation of the last P of each run.

```

dir = 0 ; dirs = [] ; P = P0 ; d = 10% P0
while (len(dirs)<20 or abs(mean(dirs))>0.1) :
    corr% = simulate(P,90) # Run the networks with P patterns
    dirold = dir
    dir = sign(corr% - 90)
    P += dir * d
    if d>1 and dir*dirold<0 :
        d = int(max(1,k*d + 0.5))
    elif d==1 :
        dirs := list of last 20 dir
return P

```

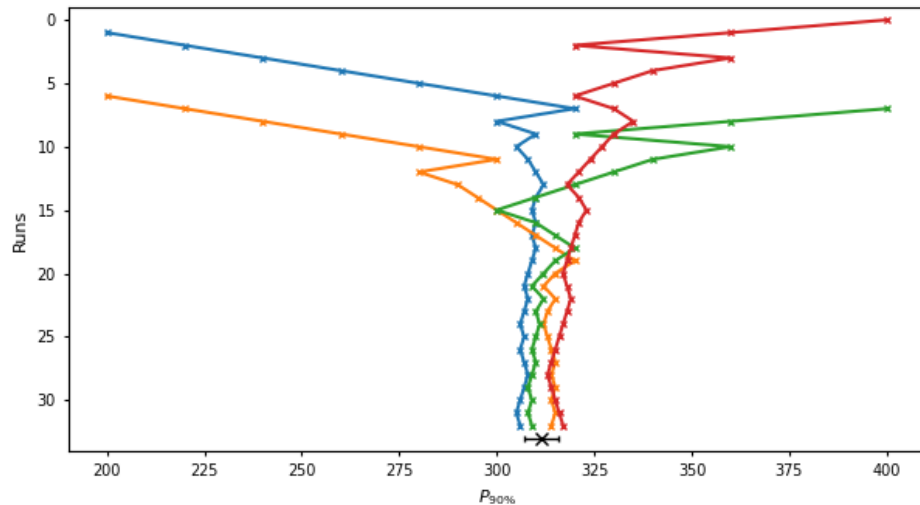


Figure S1: Estimating storage capacity. Output from the bisection method is shown with number of runs vs estimated $P_{90\%}$ for four runs of a BCPNN 16x16 network. P_0 was 200 or 400 and the pattern distortion in each run resulted from resampling 2/16 hypercolumns. The resulting estimate mean was 312 and standard deviation 4.3.